Exploring the Predictability of EEG Signals Timed with the Heartbeat: A Model-Based Approach for the Temporal and Spatial Characterization of the Brain Dynamics

Valeria Rosalia Vergara[1], Chiara Barà[1], Riccardo Pernice[1], Andrea Zaccaro[2], Francesca Ferri[3,4], Luca Faes[1], and Yuri Antonacci[1]

[1] Department of Engineering, University of Palermo, Building 9, Viale delle Scienze, Palermo, Italy
valeriarosalia.vergara@unipa.it
[2] Department of Psychological, Health and Territorial Sciences, "G. d'Annunzio" University of Chieti-Pescara, Chieti, Italy
[3] Department of Neuroscience, Imaging and Clinical Sciences, "G. d'Annunzio" University of Chieti-Pescara, Chieti, Italy
[4] Institute for Advanced Biomedical Technologies, ITAB, "G. d'Annunzio" University of Chieti-Pescara, Chieti, Italy

Abstract. This study aims to provide a temporal and spatial characterization of the human brain activity related to the cardiac cycle in terms of regularity of the brain wave amplitudes measured from electroencephalographic (EEG) signals. To achieve this objective, linear autoregressive models are employed to characterize time-series of the spectral power extracted from EEG signals, timed with the heartbeat, by using a measure of predictability. The analysis is performed on four different time-series acquired on healthy subjects in a resting state and describing the EEG spectral content over the whole frequency spectrum and within the θ, α and β bands. Our results indicate predictability values with targeted activations in the frontal and parieto-occipital brain regions, which reflect regular amplitude modulations of the brain waves at rest, and could be linked to the cortical processing of the heartbeat.

Keywords: EEG signals, spectral analysis, predictability

1 Introduction

Electroencephalography (EEG) is a non-invasive and portable technique that provides high temporal resolution for recording and analyzing the electrical activity of the brain. This method allows the study of brain dynamics and their interactions with other physiological systems in the human body [1]. One promising approach for exploring such interactions is Network Physiology, which considers the body as a network of multiple interacting complex systems [2,3]. Among the various interactions between different organ systems, investigating

the brain-heart interplay can offer valuable insights into the intricate relationship between the cardiovascular system and the brain. Several studies suggest that heart timing optimizes numerous neural processes related to homeostatic and allostatic regulation [4]. The reciprocal influence of each organ's activity on the other, exerted through neural and hormonal pathways, leads to constant bidirectional communication between the brain and the heart, with several cortical regions playing a key role in the link between sensory and visceral-motor function [5]. Therefore, studying the cortical processing of the heartbeat may provide significant implications for our understanding of perceptual, cognitive, and emotional processes.

In the literature, one approach to studying the cortical processing of the cardiac signal is the Heartbeat Evoked Potential (HEP) [6]. In this approach, EEG traces are segmented and timed with respect to the electrocardiogram (ECG) R-peak, and the relative potential is obtained through averaging. However, this approach does not provide any detail about the information content of the analyzed signal. Recently, an alternative approach based on studying the regularity of the EEG signal in different phases of the cardiac cycle was introduced to study the heartbeat-evoked responses from a different perspective [7]. Both approaches aim to investigate brain-heart interactions focusing on the impact that the heartbeat has on the EEG dynamics. However, neither approach allows for an assessment of EEG predictability in the frequency domain, which would be desirable given the abundance of oscillatory content of EEG signals.

The aim of this study is to characterize the predictability of the overall EEG spectral power, as well as of the power of the different EEG waves, when it is timed to the heartbeat. To accomplish this, we considered multiple time-series representing the changes of the EEG variance and of the EEG spectral content within the θ, α and β bands [8], over several consecutive cardiac cycles. These time series were extracted in eighteen healthy individuals monitored in a resting condition, and were analyzed exploring their statistical properties over the scalp, via the computation of mean and standard deviation, as well as of their predictability based on linear autoregressive models.

2   Materials and methods

2.1   Dataset description and pre-processing

Eighteen healthy individuals, aged between 25 and 50 years, were simultaneously monitored via EEG and ECG signals in a resting-state condition for about 10 minutes. The dataset comprises signals from 60 EEG channels (using the 10-20 system and referencing FC_Z), as well as an ECG trace acquired via a one-lead system, both of which were sampled at a frequency of $2kHz$ [6]. EEG signals were band-pass filtered (0.5 - 40 Hz, FIR filter, Hamming window), visually inspected and corrected both manually and through the FastICA (Independent Component Analysis) algorithm for removing artifacts and finally down-sampled to 128 Hz [6].The R peaks from the ECG signals were detected with a modified version of the Pan-Tompkins algorithm.

2.2   Time-series extraction

Let us consider a zero-mean stationary stochastic process X and the present state of this process as the random variable which samples X at time n, i.e. $X_n, n \in \mathbb{Z}$. In the frequency domain, this process can be described on the basis of its Power Spectral Density (PSD) defined as the Fourier Transform (FT) of the auto-correlation function of the process $P_X(\omega) = F\{r_X(k)\}, r_X(k) = \mathrm{E}[X_n X_{n-k}]$ with k representing the time lag and $\omega \in [-\pi, \pi]$ the normalized sampling frequency ($\omega = 2\pi \frac{f}{f_s}$ with $f \in [-\frac{f_s}{2}, \frac{f_s}{2}]$, f_s sampling frequency). Directly from the Wiener-Khinchine theorem for discrete time processes, the following relation holds: $\sigma_X^2 = r_X(0) = \frac{1}{2\pi} \int_{-\pi}^{\pi} P_X(\omega)d\omega$, indicating that the variance of the process X is equal to the integral of its PSD over the whole frequency spectrum [9]. In this work, the PSD was estimated through the weighted covariance (WC) method, which represents a non-parametric approach for deriving the PSD through the FT of the sample autocorrelation function of the data [9]. The WC estimator computes the PSD of the process X as

$$\hat{P}_X(\omega) = \sum_{k=-\tau}^{\tau} w(k)\hat{r}_X(k)e^{-j\omega k}; \tag{1}$$

where $\tau \leq N - 1$ is the maximum lag for which the correlation is estimated (with N being the number of data samples available), and w is a lag window of width 2τ ($w(k) = 0$ for $|k| > \tau$) which is normalized ($0 \leq w(k) \leq w(0) = 1$) and symmetric ($w(-k) = w(k)$) [9]. Window selection is usually performed by looking at the spectral leakage introduced by the profile of the window [10]. In this work, we used a biased estimator for the autocorrelation function, which guarantees semi-definite sequences and thus does not lead to negative spectral estimates. The biased estimator of the cross-correlation function is

$$\hat{r}_X(k) = \frac{1}{N} \sum_{n=0}^{N-1-k} X_n^* X_{n+k}, \tag{2}$$

where the latter holds for $k = 0, \ldots, N - 1$; if $k = -(N - 1), \ldots, -1$, the auto-covariance matrix is defined as $\hat{r}_X(k) = \hat{r}_X^*(-k)$.

To obtain the time series representing the variations of the amplitude of the various EEG rhythms, the PSD was computed on the recorded EEG signals using the WC method (Hamming window, $\tau = 64$). Specifically, the PSD was first estimated for each EEG epoch identified as the window between two consecutive R peaks in the ECG trace (as depicted in Fig.1a). Then, for each window, an estimate of the amplitude of the θ, α and β brain waves was obtained averaging the PSD profile within the frequency bands $(4-8)$ Hz, $(8-13)$ Hz, and $(13-33)$ Hz. The time series describing the variations in time of the total EEG power, computed as the variance of the signal in each considered RR interval, was also considered. With this procedure, four synchronous time series of length $N = 300$ (P_{EEG}, $P_{EEG\theta}$, $P_{EEG\alpha}$ and $P_{EEG\beta}$) were obtained from each sampled EEG signal and for each subject (Fig.1b).
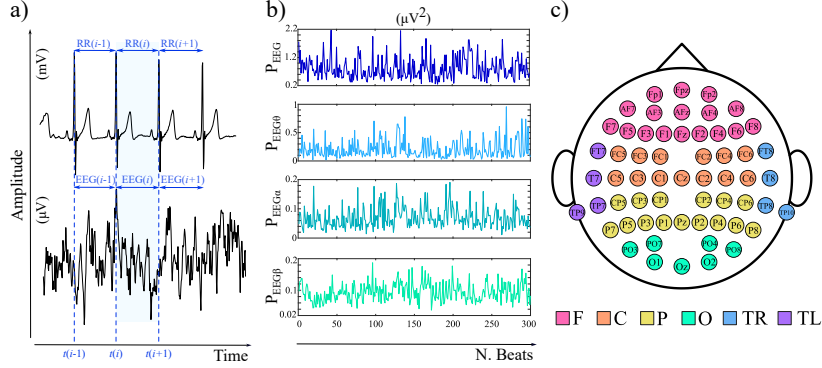
Fig. 1. (a) Example of ECG (top) and one-channel EEG (bottom) signals of one representative subject. Each heartbeat window is identified between two consecutive ECG R peaks, i.e., within each RR-interval, RR(i), with i indicating the considered R-peak. (b) Example of the four time-series extracted: total power (P_{EEG}) and power of spectral band components θ ($P_{EEG\theta}$), α ($P_{EEG\alpha}$), β ($P_{EEG\beta}$). (c) Overview of the EEG electrode montage according with the international standard 10/20 highlighting the position of the 60 EEG electrodes covering the scalp of the subjects with the specification of the 6 different brain areas selected (frontal (F), central (C), parietal (P), occipital (O), right-temporal (TR), left-temporal (TL)).

2.3   Time-series characterization

Let us consider a discrete-time, zero-mean stationary stochastic process Y, whose present state is represented by the scalar variable Y_n . Assuming that Y_n is a Markov process of order p, its past history (Y_n^-) can be approximated with p lags, i.e., $Y_n^- \simeq Y_n^p = [Y_{n-1}, \ldots, Y_{n-p}]^\top \in R^{p \times 1}$. In the linear signal processing framework, the dynamics of the process Y can be described by using the following Autoregressive (AR) model:

$$Y_n = \mathbf{A}Y_n^p + U_n, \tag{3}$$

where $\mathbf{A} = [a_1, \ldots, a_p] \in R^{1 \times p}$ is the vector of the AR coefficients and U_n is a zero-mean white Gaussian innovation process with variance $\sigma_U^2 \equiv \mathrm{E}[U_n U_n^\top]$. In this context a simple and useful measure for describing the dynamics of a univariate stochastic process is the predictability, computed as the squared version of Pearson's correlation coefficient [11]:

$$\rho_{Y_n Y_n^p}^2 = 1 - \frac{\sigma_U^2}{\sigma_Y^2}. \tag{4}$$

This is a measure of self-predictability quantifying the portion of the variance of Y that can be predicted from the exclusive knowledge of its own dynamics and is also inversely related to the complexity of the time series [12]. While the variance of the process Y can be directly computed from the time series,

the innovation variance σ_U^2 can be estimated via the identification procedure of the AR model (3) that is typically performed through the well-known Ordinary Least Square (OLS) method [12]. In brief, considering N consecutive time steps, a compact representation of the AR model (in Eq. (3)) can be defined as $y = \mathbf{A}y^p + U$, where $y = [Y_{p+1}, \ldots, Y_N]$ and $U = [U_{p+1}, \ldots, U_N]$ are the $1 \times (N - p)$ vectors and $y^p = [\mathbf{Y}_{p+1}^p, \ldots, \mathbf{Y}_N^p]$ is a $p \times (N - p)$ matrix collecting the regressors terms. The method estimates the coefficient vector through the OLS formula: $\hat{\mathbf{A}} = y(y^p)^\top[y^p(y^p)^\top]^{-1}$; then, the innovation process is estimated as the residual time-series $\hat{U} = y - \hat{\mathbf{A}}y^p$, whose variance $\hat{\sigma}_U^2$ is an estimate of the innovation variance. It is worth of note that in this work we used a logarithmic version of the squared correlation coefficient as defined in Eq. (4) that under the Gaussian assumption is related to the well known measure of Information Storage [12].

The logarithmic predictability measure was used for characterizing the EEG signals timed with heartbeat in terms of regularity. The measure was computed on the four time-series for each subject and each of the 60 EEG channels considered. The optimal model order p was estimated through the Akaike Information Criteria (AIC) ($p=3.0846\pm2.3614$).

The statistical significance of each computed predictability measure was assessed using surrogate data. Specifically, surrogates of each analyzed power time series were constructed by randomizing the order of the data in the series, thus destroying the relationship between their present and past states. The procedure was repeated 100 times, for each time-series, EEG channel and for each subject, estimating the predictability value at each iteration. The value of predictability computed on the original series was then compared with a threshold set at the 95th percentiles of the distribution of predictability values computed on the surrogates, and the original value was considered statistically significant when it was above this threshold.

2.4   Statistical analysis

For each EEG channel and for each subject, the four different time-series (P_{EEG}, $P_{EEG\theta}$, $P_{EEG\alpha}$, $P_{EEG\beta}$) were averaged over the 300 cardiac cycles analyzed to obtain MEAN value. This process was then repeated to obtain the standard deviation of each time-series, indicated as SD. Concerning the predictability analysis, one value was obtained for each EEG channel and each subject directly from the estimation procedure described in the previous section. This resulted in a distribution of each parameter (i.e., average value (MEAN), standard deviation (SD) and predictability measure (RHO)), for each electrode and for each time series across the 18 subjects. Since, the null hypothesis of normality of the Shapiro-Wilk test was rejected for more than 50% of electrodes, non-parametric statistics were used.

To determine if there were any changes in EEG activity, we assessed the modulation of a specific parameter (MEAN, SD, or RHO) in each EEG channel across three frequency bands (θ, α, and β). Paired samples Wilcoxon tests were used to compare the distributions of each parameter across frequency bands. To correct for multiple comparisons, we applied a Bonferroni correction with n=3.

We also analyzed spatial variations across the scalp by identifying six regions based on the electrode locations shown in Figure 1.c: frontal (F), central (C), parietal (P), occipital (O), right-temporal (TR), and left-temporal (TL). For each subject and time series, we calculated the mean of the MEAN, SD, and RHO parameters for each region by averaging the values from all the electrodes in that region. We then used Wilcoxon tests for independent data to compare pairs of brain regions. To correct for multiple comparisons, we used a Bonferroni correction with n=15.

3   Results

Figure 2.a-b shows the scalp distributions of the MEAN and SD parameters obtained from each time-series, averaged across participants, along with the corresponding boxplots reporting the distributions of their average values computed across electrodes belonging to the same brain regions identified in Fig. 1.c.

Figure 2.a and Figure 2.b show similar distributions of mean power and its variability values over the scalp. The θ rhythm exhibits the most homogeneous scalp activity, with the lowest values of MEAN and SD. Higher frequency spectral components tend to have less uniform distribution. Specifically, the α rhythm appears to have the greatest impact on EEG activity, with a distribution superimposed on that of total power, and the highest values localized in the parieto-occipital regions. Conversely, the β rhythm displays higher mean power activity in the fronto-occipital regions. The scalp distributions reveal apparent differences between groups of electrodes; however, the statistical analysis comparing the distributions of MEAN and SD across different scalp regions does not confirm these differences, as shown by the boxplots presented at the bottom of panels a and b. Figure 2.c-d present the results of the statistical analysis comparing the distributions of the MEAN and SD parameters between pairs of frequency bands for each scalp electrode across the 18 subjects. The average spectral power in α and β bands is significantly higher than that in the θ band across most of the scalp areas, with the exception of the frontal region. In contrast, the SD is greater in the α band, resulting in significant differences when compared to θ and β bands across the entire scalp (Figure 2.d).

Figure 3.a shows the scalp distributions of the RHO parameter obtained from each analyzed time-series, averaged across the 18 participants. The α and β rhythms exhibit the highest RHO values, and their spatial patterns overlap with those observed in the total power time-series, with the highest predictability values in the frontal and parieto-occipital brain regions. However, when comparing RHO distributions across brain regions (Fig. 3.b), no statistically significant differences are found.

Figure 3.c displays the results of a statistical analysis comparing the RHO parameter distributions across subjects for different frequency bands in each scalp electrode. The results confirm the presence of statistically significant higher predictability values in α and β bands compared to the θ band. These statistical significances are distributed across almost all the scalp, with the exception of
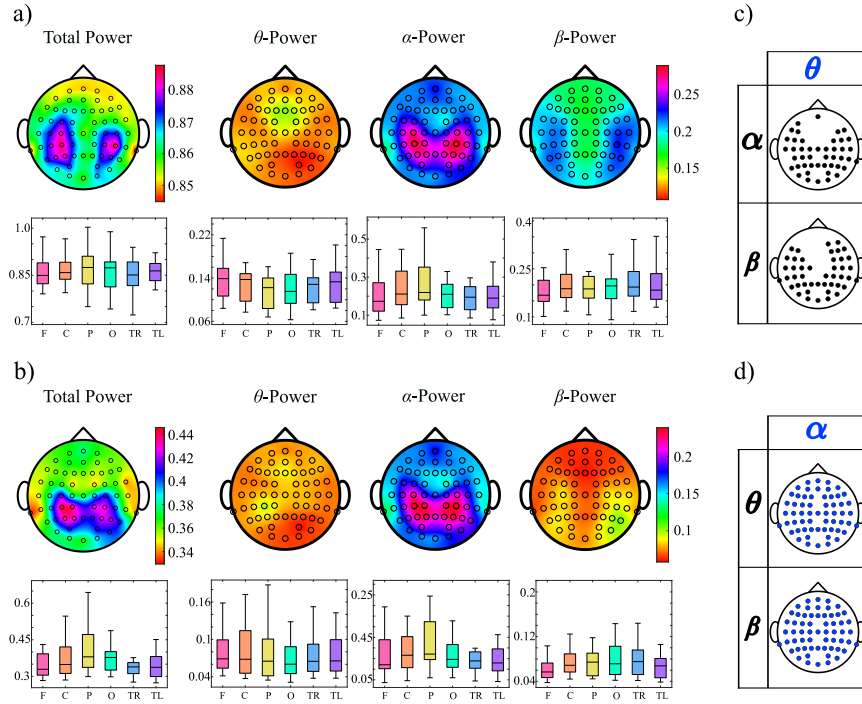
Fig. 2. Scalp distributions of the average values across subjects of MEAN (a) and SD (b) for the four time-series (expressed in μV^2) with the corresponding distributions across participants of their average values over the six brain regions (frontal (F), central (C), parietal (P), occipital (O), right-temporal (TR), left-temporal (TL)), reported as box plots. Results of the statistical analysis performed by comparing, for a given electrode, MEAN (c) and SD (d) of the time-series θ,α and β. Wilcoxon test; Bonferroni correction ($\alpha = 0.05/3$). Given two generic frequency bands r_i (row) and r_j (column), black filled circles on a specific position over the scalp denote that r_i is statistically significantly greater than r_j. For the opposite scenario blue filled circles are used.

the frontal, central, and left-parietal brain regions for comparisons between β and θ bands, which do not show any statistically significant differences.

Figure 4 presents the results of surrogates analysis to determine the statistical significance of predictability measure calculated for each time-series. The time-series were grouped by brain regions, and the overall results are summarized using barplots. The results demonstrate that, with the exception of the time-series representing average power in the θ band, the predictability of the remaining time-series show statistical significance in approximately 50% of subjects, regardless of the brain region considered. The parieto-occipital regions exhibit the highest values of statistical significance for both total and α power.
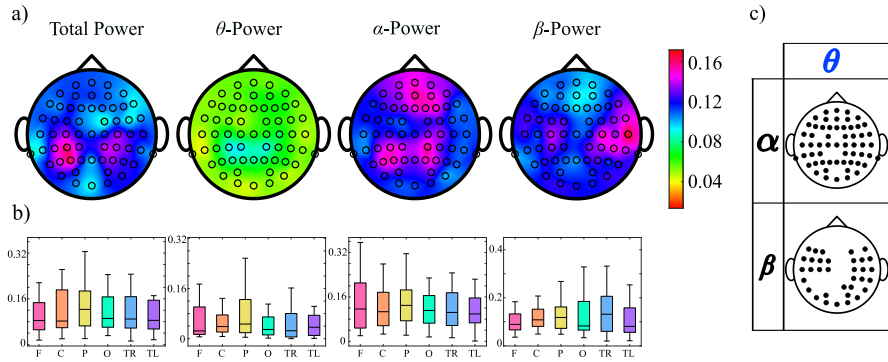
Fig. 3. (a) Scalp distributions of the mean values, computed in the population of participants, of the predictability measure (expressed in *nats*) computed for the four time-series (total power, θ, α, β powers). (b) Boxplots reporting the distributions across participants of the predictability measure averaged in the six brain regions (frontal (F), central (C), parietal (P), occipital (O), right-temporal (TR), left-temporal (TL)). (c) Results of the statistical analysis performed to compare the distributions across participants of the RHO values in different frequency bands for a given electrode. Given two generic frequency bands r_i (row) and r_j (column), black filled circles on a specific position over the scalp denote that r_i is statistically significantly greater than r_j by using the Wilcoxon signed-rank test with Bonferroni correction ($\alpha = 0.05/3$).

However, this trend is not observed for the β band, which shows a homogeneous distribution of statistical significance across different brain regions.
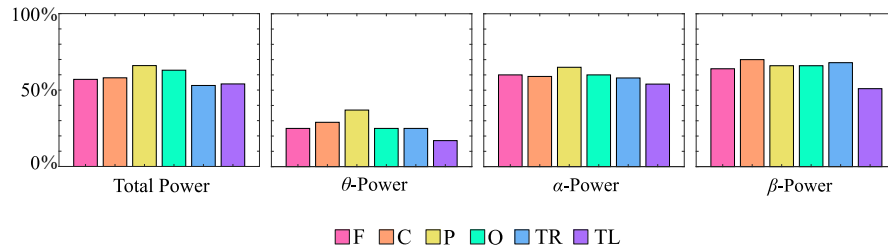

Fig. 4. Bar plots reporting the average percentage significance values across electrodes belonging to the same regions, for the four time-series analyzed.

4   Discussion

This study aimed to explore the spatiotemporal distributions of various statistical parameters, including mean, standard deviation, and predictability, computed over distinct time-series representing the frequency content of EEG signals evaluated at the time scale of the cardiac cycle. The study employed a non-parametric approach to estimate the PSDs of brain signals in a cohort of 18 healthy participants at resting-state. Our investigation focused primarily on the frequency bands known to be relevant to the brain activity, namely θ, α, and β, as well as the total power of the EEG signals.

The analysis of MEAN and SD parameters shown in Figure 2 reveals an homogeneous distribution of these parameters over the scalp, documented together with a prominent activity in the α frequency band, which demonstrates to be the largest contribution to the total power. As several studies report, it is well known that prominent brain activity in the α band in the parieto-occipital region is expected during a resting phase with eyes open [1, 13]. As depicted in Fig. 3, this observation may suggest a more regular activity of the brain promoted by the activation of the default mode network, whose activity has been associated in the literature with an increase in EEG power in the α and β frequency bands in parietal and occipital regions [14]. Investigations of heartbeat cortical processing via HEP highlighted similar targeted activations in these regions [15]. As regards the regularity of the time series of brain wave amplitude, we find that the time series of α and β brain wave amplitudes displays the higher levels of predictability. This is also confirmed by the analysis of the significance of the predictability computed on the time-series extracted from the EEG signals and shown in Figure 4 which highlights the maximum significance level reaching approximately 50% only in the parieto-occipital regions for the total power, for the power in α band, and for the β power over the whole scalp.

Although a spatial pattern for the MEAN, SD, and RHO parameters when computed for the total power and the spectral content in the α band is evident in the results, there are no statistically significant differences observed among the various brain regions. However, a thorough analysis of the results shown in Figures 2 and 3 reveals specific trends where parieto-occipital regions appear to be more involved, irrespective of the statistical measure used. While lack of statistical significance could be due to the presence of high inter-subject variability at rest, leading to a high standard deviation in the analyzed distributions [16], the current results indicate that the mechanisms determining the occurrence of predictable brain wave amplitudes are not region-specific.

5   Conclusions

This study introduced an approach for characterizing the brain dynamics by extracting amplitude variability time series of brain rhythms measured at a time scales compatible with the heart rhythm. The time series were analyzed by examining their average and variability values, as well as their predictability.

The results show a greater regularity in the amplitude modulations of the α and β brain waves, suggesting that these rhythms could be more involved in the cortical processing of the heartbeat in the resting state. Although these findings are consistent with other studies in the literature, it is important to note some limitations. These include the relatively low significance of the predictability measure, the small sample size, and the use of a linear estimator that may not detect possible non-linear behaviors.

This study should be considered as a starting point for future investigations focusing on bidirectional analysis of brain-heart interactions and aimed to better understand the underlying physiological mechanisms of brain-heart interplay. We suggest that these interactions should be investigated primarily looking at the correlation between α and β brain wave amplitudes and heart rate variability.

Acknowledgement

References

1. L. Faes, D. Marinazzo, G. Nollo, and A. Porta, "An information-theoretic framework to map the spatiotemporal dynamics of the scalp electroencephalogram," *IEEE Transactions on Biomedical Engineering*, vol. 63, no. 12, pp. 2488–2496, 2016.
2. P. C. Ivanov, "The new field of network physiology: building the human physiolome," *Frontiers in Network Physiology*, p. 1, 2021.
3. C. Schmal, S. Hong, I. Tokuda, and J. Myung, "Coupling in biological systems: Definitions, mechanisms, and implications," 2022.
4. D. Candia-Rivera, "Brain-heart interactions in the neurobiology of consciousness," *Current Research in Neurobiology*, p. 100050, 2022.
5. D. Azzalini, I. Rebollo, and C. Tallon-Baudry, "Visceral signals shape brain dynamics and cognition," *Trends in cognitive sciences*, vol. 23, no. 6, pp. 488–509, 2019.
6. A. Zaccaro, M. G. Perrucci, E. Parrotta, M. Costantini, and F. Ferri, "Brain-heart interactions are modulated across the respiratory cycle via interoceptive attention," *Neuroimage*, vol. 262, p. 119548, 2022.
7. C. Barà, A. Zaccaro, Y. Antonacci, M. Dalla Riva, A. Busacca, F. Ferri, L. Faes, and R. Pernice, "Local and global measures of information storage for the assessment of heartbeat-evoked cortical responses," *[Manuscript submitted for publication]*, 2022.

8. S. Schulz, M. Bolz, K.-J. Bär, and A. Voss, "Central-and autonomic nervous system coupling in schizophrenia," *Philosophical Transactions of the Royal Society A: Mathematical, Physical and Engineering Sciences*, vol. 374, no. 2067, p. 20150178, 2016.

9. S. Kay, "Spectral estimation," *Advanced topics in signal processing*, pp. 58–122, 1988.

10. Y. Antonacci, L. Minati, D. Nuzzi, G. Mijatovic, R. Pernice, D. Marinazzo, S. Stramaglia, and L. Faes, "Measuring high-order interactions in rhythmic processes through multivariate spectral information decomposition," *IEEE Access*, vol. 9, pp. 149 486–149 505, 2021.

11. G. Chiarion, L. Sparacino, Y. Antonacci, L. Faes, and L. Mesin, "Connectivity analysis in eeg data: A tutorial review of the state of the art and emerging trends," *Bioengineering*, vol. 10, no. 3, p. 372, 2023.

12. L. Faes, D. Marinazzo, S. Stramaglia, F. Jurysta, A. Porta, and N. Giandomenico, "Predictability decomposition detects the impairment of brain–heart dynamical networks during sleep disorders and their recovery with treatment," *Philosophical Transactions of the Royal Society A: Mathematical, Physical and Engineering Sciences*, vol. 374, no. 2067, p. 20150177, 2016.

13. C. Babiloni, G. Binetti, A. Cassarino, G. Dal Forno, C. Del Percio, F. Ferreri, R. Ferri, G. Frisoni, S. Galderisi, K. Hirata *et al.*, "Sources of cortical rhythms in adults during physiological aging: a multicentric eeg study," *Human brain mapping*, vol. 27, no. 2, pp. 162–172, 2006.

14. C. D. B. Luft and J. Bhattacharya, "Aroused with heart: Modulation of heartbeat evoked potential by arousal induction and its oscillatory correlates," *Scientific reports*, vol. 5, no. 1, p. 15717, 2015.

15. G. Dirlich, T. Dietl, L. Vogl, and F. Strian, "Topography and morphology of heart action-related eeg potentials," *Electroencephalography and Clinical Neurophysiology/Evoked Potentials Section*, vol. 108, no. 3, pp. 299–305, 1998.

16. S. I. Gonçalves, F. Bijma, P. J. Pouwels, M. A. Jonker, J. P. Kuijer, R. M. Heethaar, F. H. L. Da Silva, and J. C. De Munck, "Inter-subject variability of resting state brain activity explored using a data and model-driven approach in combination with eeg-fmri," in *2008 5th IEEE International Symposium on Biomedical Imaging: From Nano to Macro.* IEEE, 2008, pp. 608–611.